

1 Selection against archaic hominin genetic variation in
2 regulatory regions

Natalie Telis¹, Robin Aguilar², and Kelley Harris^{1,2,3}

¹Department of Genetics, Stanford University

²Department of Genome Sciences, University of Washington

³Fred Hutchinson Cancer Research Center, Computational Biology Division

3 Correspondence: natalie.telis@gmail.com, harriske@uw.edu

4 June 24, 2020

5

Abstract

6
7
8
9
10
11
12
13
14
15
16
17
18
19
20
21
22
23
24
25
26
27
28
29
30

Traces of archaic hominin DNA persist in the human gene pool, but are systematically depleted around genes and other functionally important genomic regions. This suggests that many Neandertal and Denisovan alleles had harmful effects on hybrid fitness. We hypothesized that if some harmful effects were mediated by gene dysregulation in specific tissues, alleles previously flagged as archaic using a conditional random field (CRF) should be depleted from those tissues' regulatory enhancers compared to "control" alleles matched for allele frequency and the strength of background selection. By this metric, both Neandertal and Denisovan variation appear depleted from enhancers, particularly enhancers that show pleiotropic activity across tissues. This depletion is driven by young archaic SNPs that the CRF confidently identifies as private to Neandertals or Denisovans; older variants that were likely present in both archaic species are not depleted from enhancers. We found that enhancer pleiotropy is not only a predictor of archaic SNP depletion, but also a predictor of intolerance to new mutations as measured by both phastCons scores and the frequency spectrum of African variation. In other respects, however, the landscape of selection against young archaic alleles appears qualitatively different from the landscape of ordinary purifying selection, suggesting that archaic alleles had a different distribution of fitness effects from ordinary new mutations. Most strikingly, fetal brain and muscle are the tissues most depleted of young archaic variation in their regulatory regions, but only brain enhancers appear commensurately intolerant to new mutations. In contrast, fetal muscle enhancers show no evidence of elevated purifying selection relative to other enhancers. This suggests that epistatic incompatibility between human and archaic alleles is needed to explain the degree of archaic variant depletion from fetal muscle enhancers, perhaps due to divergent selection for higher muscle mass in archaic hominins compared to humans.

31 Introduction

32 Although hybrids between humans and archaic hominins were once viable, fertile and nu-
33 merous [1, 2, 3, 4], Neandertal and Denisovan alleles have been systematically depleted from
34 the most functionally important regions of the human genome [5, 6, 7]. This pattern im-
35 plies that archaic introgression often had deleterious consequences for human populations,
36 but it is challenging to fine-map the locations of detrimental archaic alleles and determine
37 the nature of their fitness effects. Petr, et al. recently found that promoters were actually
38 more depleted of introgression than the coding sequences that lie immediately downstream,
39 lending weight to the longstanding hypothesis that gene regulatory mutations underlie much
40 of the functional divergence between closely related lineages of hominins [8, 9, 10]. Two
41 other recent studies found that introgressed alleles are associated with gene expression vari-
42 ation more often than expected by chance [11, 12], implying that even the archaic regulatory
43 variation that remains in the human gene pool is not necessarily benign.

44 Previous work showed that selection was likely relaxed within the Neandertal exome,
45 leading the accumulation of deleterious mutations, by comparing rates of amino acid change
46 to rates of substitution at synonymous sites [13]. However, it is less straightforward to
47 perform similar analyses on noncoding variation because of gaps in our understanding of
48 the grammar relating sequence to regulatory function [14, 15]. Allele frequency spectra
49 and patterns of sequence divergence can sometimes provide information about the mode
50 and intensity of selection acting on noncoding regions [16, 17, 18, 19, 20], but introgressed
51 variants have an unusual distribution of allele ages and frequencies that can confound the
52 efficacy of standard methods that assume simple population histories [21]. Reporter assays
53 can directly measure the impact of archaic variants on gene expression *in vitro* [22, 23, 24],
54 but they cannot translate gene expression perturbations into the subtle effects on survival
55 and reproduction that likely determined which archaic variants were purged from human
56 populations.

57 Petr et al. used a direct f_4 ratio test to conclude that promoters and other conserved
58 noncoding elements harbored less Neandertal DNA than the genome as a whole, but found
59 no similar depletion in enhancers. However, a subsequent study by Silvert et al. came
60 to somewhat different conclusions using different methodology, which involved quantifying
61 the distribution of alleles flagged as likely Neandertal in origin based on their presence in
62 the Altai Neanderthal reference and their absence from an African reference panel [25].

63 Most such alleles are presently rare (<2% frequency in modern Eurasians), and Silvert, et
64 al. found these rare archaic alleles to be significantly depleted from enhancers. However,
65 archaic variants present at population frequencies of 5% or more were found to occur in
66 enhancers more often than expected by chance. Enhancers containing these common archaic
67 alleles were found to be preferentially active in T cells and mesenchymal cells, perhaps due
68 to positive selection for alleles that alter gene expression in the immune system [25].

69 The results of these two prior papers are consistent with a model in which most intro-
70 gressed enhancer sequences have been segregating neutrally within the human gene pool,
71 but in which archaic haplotypes containing private Neandertal enhancer variation were more
72 often selected against than introgressed haplotypes containing private Neandertal variants
73 outside regulatory regions. To interrogate this model more directly, we leverage a set of
74 archaic variant calls that were previously generated using a conditional random field (CRF)
75 approach [5, 7]. The CRF introgression calls are hierarchically organized in a way that cor-
76 relates with age: some of these alleles are confidently inferred to be either Neandertal or
77 Denisovan in origin, while others might have originated in either archaic species and likely
78 segregated for a longer period of time prior to human secondary contact. We quantify the
79 abundance of young versus old archaic alleles in enhancers as a function of tissue activity,
80 controlling for the amount of background selection enhancers experience, to estimate whether
81 selection likely acted to remove certain classes of archaic variants from regulatory regions.

82 Results

83 **Enhancers appear depleted of Neandertal alleles compared to control regions** 84 **affected by similar levels of background selection**

85 We intersected the ENCODE Roadmap enhancer calls with the high confidence Neander-
86 tal and Denisovan SNP calls generated from the Simons Genome Diversity Panel (SGDP)
87 [7, 26]. Of the two available call sets, we used variant set # 2, which identifies Eurasian
88 variants as Neandertal if they appear more similar to the Altai Neandertal reference than to
89 either an African reference panel or the Altai Denisovan reference. (Similarly, variants are
90 identified as Denisovan if they appear more similar to the Altai Denisovan reference than to
91 an outgroup consisting of Africans plus the Altai Neandertal reference).

92 Since Neandertal variants in enhancers might have been purged due to linkage disequilib-
93 rium with nearby coding variants, we devised a method to measure archaic allele depletion

94 while controlling for the strength of background selection, as quantified by McVicker and
95 Green’s B -statistic [27, 5, 7]. We randomly paired each Neandertal variant with two “con-
96 trol” variants matched for both B -statistic decile and allele frequency (Figure 1A), then
97 computed the proportion of archaic versus control alleles occurring within enhancers.

98 In every population, we found that control variants occur within enhancers significantly
99 more often than introgressed variants do (Figure 1B), with depletion odds ratios ranging
100 from 0.84 to 0.91 and 95% binomial confidence intervals excluding an odds ratio of 1. As
101 expected, this method also detects negative selection against introgression in exons. Enard,
102 et al. recently used a related approach to quantify Neandertal introgression in proteins that
103 interact with viruses [28]. To ensure that the linkage structure of the archaic SNPs was not
104 contributing to this result, we sampled an alternate set of controls with a similar linkage
105 block structure; upon substituting these controls for our originally sampled controls, we
106 observed a nearly identical landscape of introgression depletion (Figure S1.1).

107 **Highly pleiotropic enhancers harbor fewer archaic variants than tissue-specific** 108 **enhancers**

109 The enhancers annotated by RoadMap exhibit wide variation in tissue specificity. Some
110 are active in only one or two tissues, while others show activity in 20 tissues or more [29].
111 When we stratified enhancers by pleiotropy number, meaning the number of tissues where
112 the enhancer is active (Figure 2), we found pleiotropy to be correlated with the magnitude
113 of archaic variation depletion (Figure 2).

114 If high-pleiotropy enhancers exhibited high sequence similarity between humans, Nean-
115 dertals, and Denisovans, this could make it hard to detect archaic introgression in these
116 regulatory regions and create the false appearance of selection against introgression. How-
117 ever, we found that the human and archaic reference sequences were actually more divergent
118 in high-pleiotropy enhancers than in other regions (Figure S2.1), making selection against
119 introgression more likely to be responsible for the observed depletion gradient. Enhancer
120 activity is known to increase the mutation rate by inhibiting DNA repair [30, 31], which
121 may explain why highly active enhancers have been diverging between hominid species at
122 an accelerated rate.

123 We found substantial variation between tissues in the magnitude of archaic SNP depletion
124 (Figure 3A; Figure S3.1), as well as correlation across tissues between depletion of Neandertal
125 variants and depletion of Denisovan variants ($r^2 = 0.537$, $p < 4e-5$). Enhancers active in

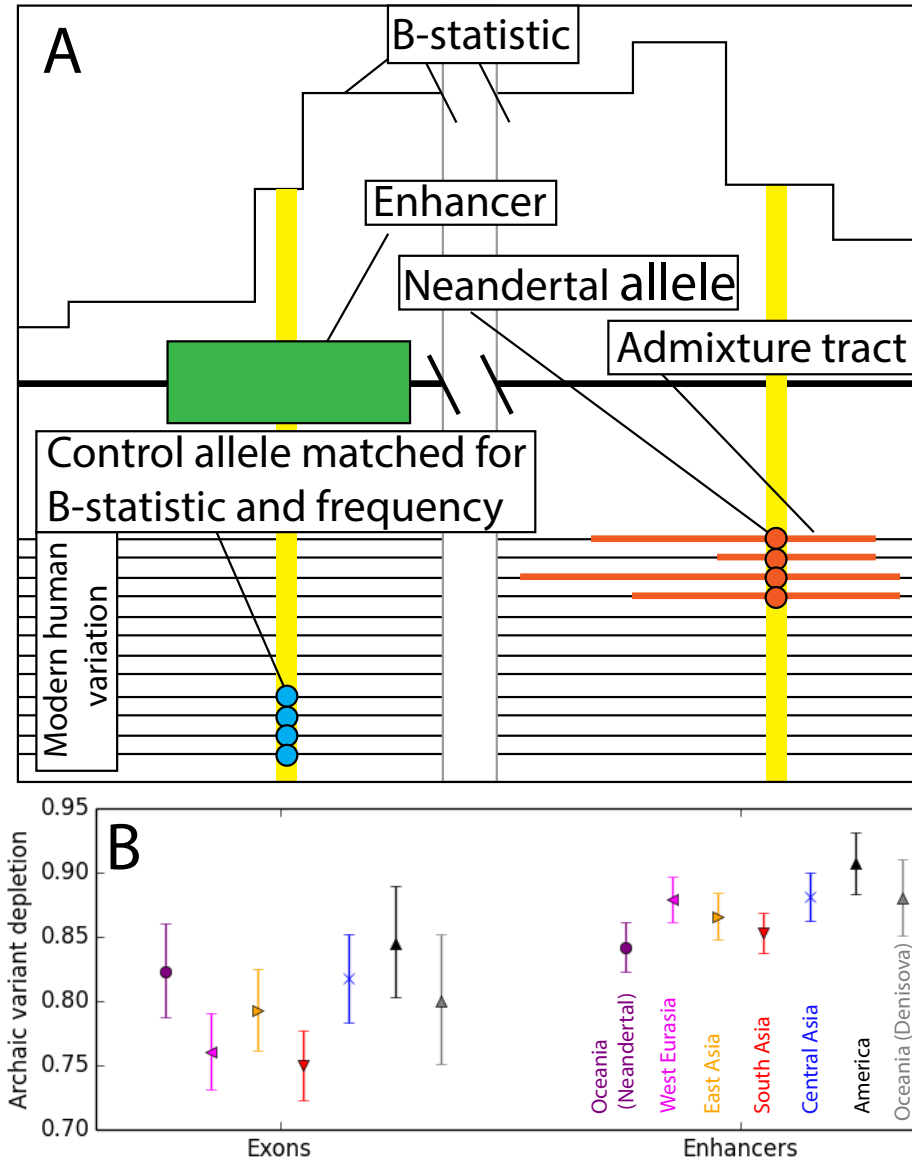


Figure 1: A. This schematic illustrates the process of matching archaic variants to “control” variants with identical allele frequencies and B statistic values. B. Introgressed-to-control variant odds ratios show depletion of Neandertal variants from both exons and enhancers in every population sequenced by the Simons Genomic Diversity Project. In the case of Oceanians, a similar pattern holds for Denisovan variant calls. Error bars span 95% binomial confidence intervals.

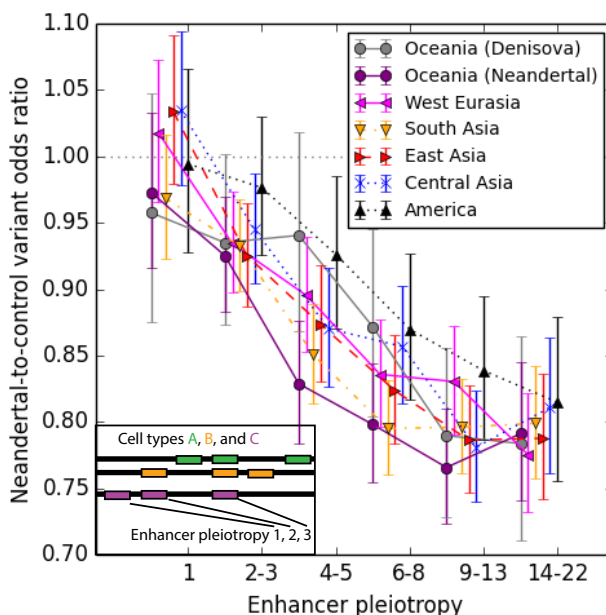


Figure 2: Enhancers active in only a single cell type do not appear depleted of archaic SNPs, whereas enhancers that are active in multiple cell types contain up to 20% fewer archaic variant calls than expected. Error bars span 95% binomial confidence intervals.

126 fetal muscle, fetal brain, and neurosphere cells are the most strongly depleted of introgressed
 127 variation, while enhancers active in fetal blood cells and T-cells, as well as mesenchymal cells,
 128 appear the least depleted. We observed no correlation across tissues between the degree of
 129 archaic variant depletion and the genetic divergence between archaic and human reference
 130 sequences (Figure S3.2). Mesenchymal cells, T-cells, and other blood cells are among the
 131 cell types where some adaptively introgressed regulatory variants are thought to be active
 132 [32, 33, 34, 25], but our results suggest that selection overall decreased archaic SNP load
 133 even within the regulatory networks of these cells. The excess archaic SNP depletion in
 134 brain and fetal muscle is a pattern that holds robustly across populations (Supplementary
 135 Figure S3.2). Although exons are slightly more depleted of archaic SNPs than enhancers as
 136 a whole (see the non-overlapping 95% confidence intervals in Figure 1B), they are actually
 137 less depleted of archaic variation than brain or fetal muscle enhancers.

138 Although fetal muscle and fetal brain enhancers are more depleted of archaic SNPs than
 139 enhancers active in other tissues, selection acting in these two tissues alone is not sufficient
 140 to explain the apparent depletion of archaic SNPs from other tissues' enhancers. When we
 141 computed the magnitude of archaic SNP depletion as a function of pleiotropy in the subset
 142 of enhancers that are active in fetal brain, fetal muscle, or both, we still found pleiotropy to

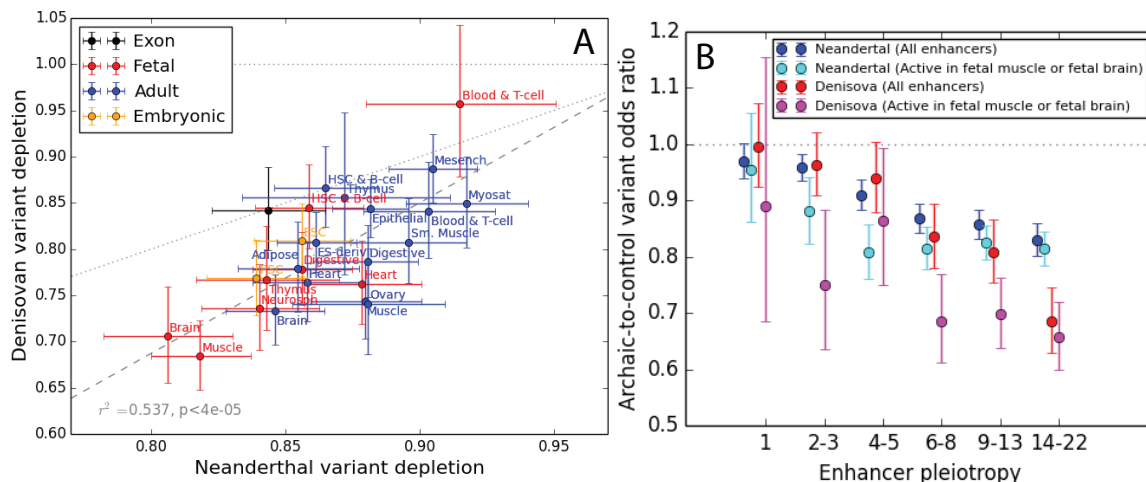


Figure 3: A. Neanderthal and Denisovan variant depletion varies between enhancers active in different tissues. Data points that lie below the dotted line correspond to tissues whose enhancers are more depleted of Denisovan SNPs compared to Neanderthal SNPs. B. Even after restricting to enhancers active in fetal muscle or fetal brain, the two tissue types most depleted of introgressed variation, pleiotropy remains negatively correlated with archaic SNP depletion. The difference between these two tissues and other tissues is driven mainly by enhancers of intermediate pleiotropy. All error bars span 95% binomial confidence intervals.

143 be predictive of introgression depletion (Figure 3B).

144 For enhancers active in 6 or more tissues, depletion of Denisovan variants is notably
 145 stronger than depletion of Neanderthal variants. One possible culprit is a discrepancy in
 146 the power of the CRF to ascertain Neanderthal versus Denisovan introgression. The Denisovans
 147 who interbred with modern humans were quite genetically differentiated from the Altai
 148 Denisovan reference individual, while the Altai Neanderthal reference is more modestly di-
 149 vergent from Neanderthal introgressed tracts [35], and this likely created differences between
 150 species in the sensitivity and specificity of archaic SNP detection.

151 **Old variation shared by Neanderthals and Denisovans was likely less deleterious**
 152 **to humans than variation that arose in these species more recently**

153 To further test the hypothesis that selection acted to purge young, rare archaic vari-
 154 ation from enhancers, we leveraged the difference between two introgression call sets that
 155 Sankararaman, et al. generated from the SGDP data [7]. As mentioned earlier, we conducted
 156 all previous analyses using “Call Set 2,” which was constructed to minimize the misidentifi-
 157 cation of Neanderthal alleles as Denisovan and vice versa. To generate Neanderthal Call Set 2,
 158 Sankararaman, et al. used an outgroup panel that contained the Altai Denisovan as well as

159 several Yoruban genomes. Similarly, Denisovan Call Set 2 was generated using a panel that
160 included Yorubans plus the Altai Neandertal. In contrast, “Call Set 1” was generated using
161 an outgroup panel composed entirely of Africans, and this procedure identifies more archaic
162 SNPs overall.

163 Compared to Set 2, we hypothesized that the more inclusive Set 1 calls should contain
164 more old variation that arose in the common ancestral population of Neandertals and Deniso-
165 vans (Figure 4A). We posited that this older variation might be better tolerated in humans
166 because it rose to high frequency in an ancestral population that was not as divergent from
167 humans as later Neandertal and Denisovan populations. Neandertals and Denisovans also
168 suffered from increasingly severe inbreeding depression as time went on, further increasing
169 the probability that younger variants could have deleterious effects [2, 13].

170 To test our hypothesis that Set 2 might be enriched for deleterious variation, we com-
171 piled sets of “old” Neandertal and Denisovan variation comprised of their respective Set 1
172 introgression calls and excluding all Set 2 introgression calls. In every population, young Ne-
173 andertal variants outnumber old Neandertal variants, but conversely, old Denisovan variants
174 outnumber young Denisovan variants (Figures 4B, S4.2). The CRF may have been better
175 powered to detect young Neandertal variants compared to young Denisovan variants due to
176 the aforementioned closer relationship of the reference Neandertal to archaic individuals who
177 interbred with humans [35]. As expected, old variants are more likely than young variants to
178 be present in both archaic reference genomes rather than just one, though more than 30% of
179 calls in each category are absent from both archaic references and are presumably identified
180 as archaic due to patterns of linkage disequilibrium (Figure 4C).

181 In contrast to the young Set 2 introgression calls, old calls are not measurably depleted
182 from enhancers compared to control variants matched for allele frequency and B statistic
183 (Figure 4D). This suggests that the introgression landscape was shaped mainly by selection
184 against Neandertal and Denisovan variants that arose relatively close to the time that gene
185 flow occurred, not variation that arose soon after their isolation from humans. Many popu-
186 lations actually show a slight enrichment of old archaic variants in enhancers compared to
187 controls, as shown in Figure 4D by 95% confidence intervals that exclude an odds ratio of
188 1. These sets of old, shared variants are possibly enriched for beneficial alleles that swept
189 to high frequency in the common ancestor of Neandertals and Denisovans. They should at
190 least be depleted of deleterious variation compared to our control alleles that likely arose

191 more recently in humans. In several cases, the odds ratio enrichment of old archaic vari-
192 ation in enhancers actually trends upward with increasing pleiotropy, possibly because the
193 highest-pleiotropy enhancers show the most divergence between human and archaic reference
194 genomes (Figure S2.1). If archaic SNPs in enhancers were generally neutral or selectively
195 favored, the positive correlation between pleiotropy and human/archaic divergence would
196 lead us to predict the odds ratio trend that is observed for old archaic variants, not the
197 opposite correlation with pleiotropy that is observed for young archaic variants.

198 Neandertals and Denisovans are thought to have begun diverging about 640,000 years
199 ago [36]. Since this is long enough to efficiently purge deleterious variation, any surviving
200 archaic variation that predates this split is likely to have nearly neutral or beneficial fitness
201 effects, assuming no negative epistasis with human variation. We can see this from a simple
202 population genetic calculation: assuming that the Neandertal/Denisovan effective population
203 size was about 4,000 [2] and their generation time is 30 years, $4Ne$ for these species would
204 be 480,000. This implies that more than half of the variation that segregated neutrally in
205 the ancestral Neandertal/Denisovan population would have been fixed or lost by the time
206 the two species interbred with humans, leaving ample time for deleterious ancestral variation
207 to be purged. 480,000 years also predates the estimate of the start of the bottlenecks that
208 affected Neandertals and Denisovans [2], so variation that predates this period may have
209 been efficiently purged of deleterious alleles that would have segregated neutrally if they
210 had arisen after the start of the bottleneck period. Some old variants might be younger
211 than the Neandertal/Denisova split if they crossed between the boundaries of these species
212 by introgression; Neandertals and Denisovans are known to have interbred with each other
213 while still maintaining distinct gene pools. This population history suggests that gene flow
214 between Neandertals and Denisovans may be enriched for variants that are benign on a
215 variety of genetic backgrounds [37], making them more likely to be benign on a human
216 background as well.

217 **Introgressed variants and recent mutations have been differently selected against** 218 **as a function of enhancer activity**

219 We next investigated whether the enhancers most depleted of young archaic variants are
220 simply the enhancers most intolerant to new mutations, leveraging the fact that natural
221 selection allows neutral and beneficial mutations to reach high frequencies more often than
222 deleterious mutations do [38, 39] (Figure 5A). Working with the site frequency spectrum

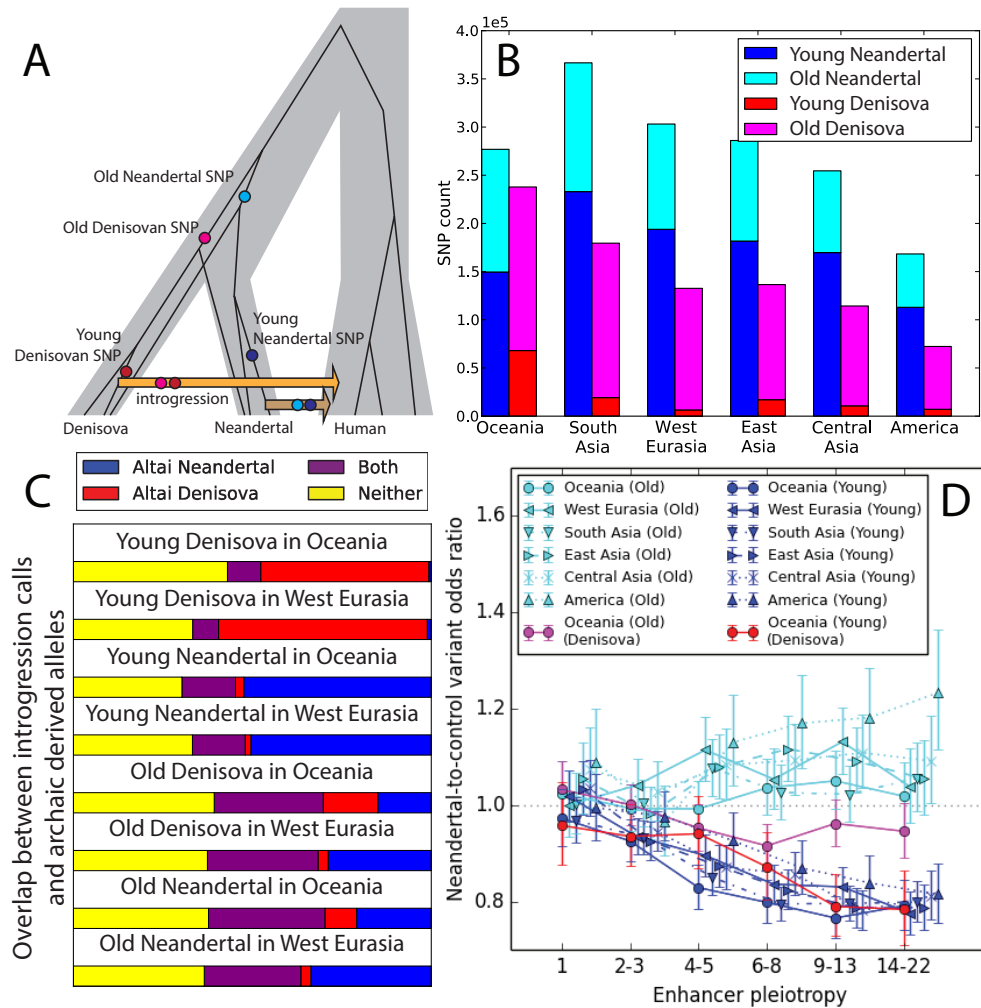


Figure 4: A. We classified introgression calls as “old” or “young” based on their presence in the Sankararaman, et al. Call Sets 1 and 2. By design, the old alleles (present in Call Set 1 but not Call Set 2) are more often shared between Neandertals and Denisovans, and we hypothesize that many of these alleles arose before the Neandertal/Denisovan divergence, as pictured, or else crossed between the two species via Neandertal/Denisovan gene flow. In contrast, we hypothesize that the young alleles most often arose after Neandertals and Denisovans had begun to diverge. B. Numerical counts of old and young introgressed variants in the SGDP human genomes. Young Denisovan variants are likely rare because the Altai Denisovan was not closely related to the Denisovan population that primarily interbred with humans [35]. C. We computed the fraction of CRF introgression calls that occur as derived alleles in the Altai Neandertal genome and/or the Altai Denisovan genome. As expected, old variants are 2-to-4-fold more likely than young variants to occur in both archaic reference genomes. See Supplementary Figures S4.1 and S4.2 for more data on allele sharing between introgression calls and the reference archaic genomes. D. In contrast to the young archaic variation considered elsewhere in this paper, old archaic variation is not measurably depleted from enhancers, even enhancers active in numerous tissues. All error bars span 95% binomial confidence intervals.

223 (SFS) of African enhancer variation from the 1000 Genomes Project, we computed the
224 proportion of variants segregating in enhancers that are singletons and compared this to the
225 proportion of singletons in the immediately upstream enhancer-sized regions (Figure 5B).
226 Neandertals contributed much less genetic material to sub-Saharan Africans compared to
227 non-Africans [1, 4], meaning that Neandertal alleles should have little direct effect on the
228 African site frequency spectrum.

229 One caveat is that this strategy will not detect the effects of strongly deleterious mutations
230 that do not segregate long enough to affect the frequency spectrum's shape. However,
231 strongly deleterious mutations are not expected to contribute to mutation load differences
232 between populations, making it appropriate to focus on identifying regions whose variation
233 is affected by selection against weakly deleterious mutations.

234 By comparing enhancers to immediately adjacent regions, we control for the potentially
235 confounding effects of recombination rate, background selection, and sequencing read depth.
236 Although enhancers likely have elevated mutation rates because transcription factor binding
237 impairs DNA repair [30], the proportion of variants that are singletons is independent of
238 mutation rate as long as the mutation rate has remained constant over time [40]. Enhancers
239 admittedly have higher GC content than adjacent control regions, but the enrichment of
240 singletons in the enhancer SFS holds separately for SNPs with AT ancestral alleles and
241 SNPs with GC ancestral alleles (Figure S5.1). This suggests that the SFS is not enriched for
242 singletons because of a force like biased gene conversion, which only depresses the frequencies
243 of mutations from GC to AT and instead increases the frequencies of mutations from AT
244 to GC [41]. There is also no apparent correlation across tissues between GC content and the
245 enrichment of rare variants in enhancers (Supplementary Figure S5.2). We conclude that
246 purifying selection is likely driving the difference between the SFSs of enhancers and control
247 regions, not base composition or biased gene conversion.

248 Although enhancers broadly show evidence of purifying selection against both archaic
249 variation and new mutations, the strength of selection against these two types of pertur-
250 bation is poorly correlated among tissues (Figure 5C, D). Although singleton enrichment
251 appears nominally correlated with Neandertal depletion ($r^2 = 0.31$, $p < 0.004$) and Denisov-
252 van depletion ($r^2 = 0.27$, $p < 0.009$), this correlation disappears when brain tissues are
253 excluded (Neandertal $p < 0.42$; Denisovan $p < 0.10$; see Figure S5.3). Fetal brain, neuro-
254 sphere cells, and, to a lesser extent, adult brain are the tissues whose active enhancers show

255 the most singleton enrichment, suggesting that mutations perturbing brain development have
256 an outsize probability of deleterious consequences. In contrast, fetal muscle enhancers show
257 no evidence of unusual selective constraint despite their strong depletion of both Neandertal
258 and Denisovan ancestry. We obtain categorically similar results when we estimate selective
259 constraint using phastCons scores rather than singleton enrichment (Figure S5.4).

260 Enhancer pleiotropy is positively correlated with singleton enrichment as well as the
261 depletion of archaic alleles (Figure 5E). This observation may be related to experimental
262 evidence that the most highly pleiotropic enhancers tend to have the most consistently
263 conserved functioning across species [42]. One difference, however, is that enhancers active
264 in only a single tissue (pleiotropy number 1) still show significant evidence of selection against
265 new mutations despite their lack of any evidence for selection against archaic introgression
266 (O.R. 95% C.I. excludes 1).

267 Discussion

268 Most methods for identifying introgressed archaic haplotypes rely on putatively unadmixed
269 outgroup data. Chen, et al. recently showed that use of an African outgroup can confound
270 measurements of introgression fraction differences between populations, causing less intro-
271 gression to be detected in Europeans compared to Asians because Europeans exchanged more
272 recent migrants with Africa [4]. Our analysis of young versus old CRF-based calls shows
273 that the choice of outgroup can also affect the distribution of archaic allele calls across
274 functional versus putatively neutrally evolving genomic regions. This implies that outgroup
275 panel use can interfere with efforts to estimate unbiased Neandertal and Denisovan admix-
276 ture fractions, but does not imply that unbiased admixture fractions are necessarily the
277 most powerful statistic for detecting the footprints of selection against archaic alleles. The
278 subset of archaic haplotypes that are most divergent from outgroup panels are by definition
279 enriched for mutations that may have detectable fitness effects, whereas archaic haplotypes
280 that are less divergent and more difficult to detect computationally are more likely to seg-
281 regate neutrally in human populations. In reaching such conclusions, proper care must be
282 taken to control for rates of human/archaic reference divergence, which can vary across the
283 genome. In enhancers, however, we found archaic/human divergence to be elevated, which
284 likely enhanced the power of the CRF to discover introgression overlapping these regions.
285 This suggests that selection is needed to explain the observed depletion of young archaic

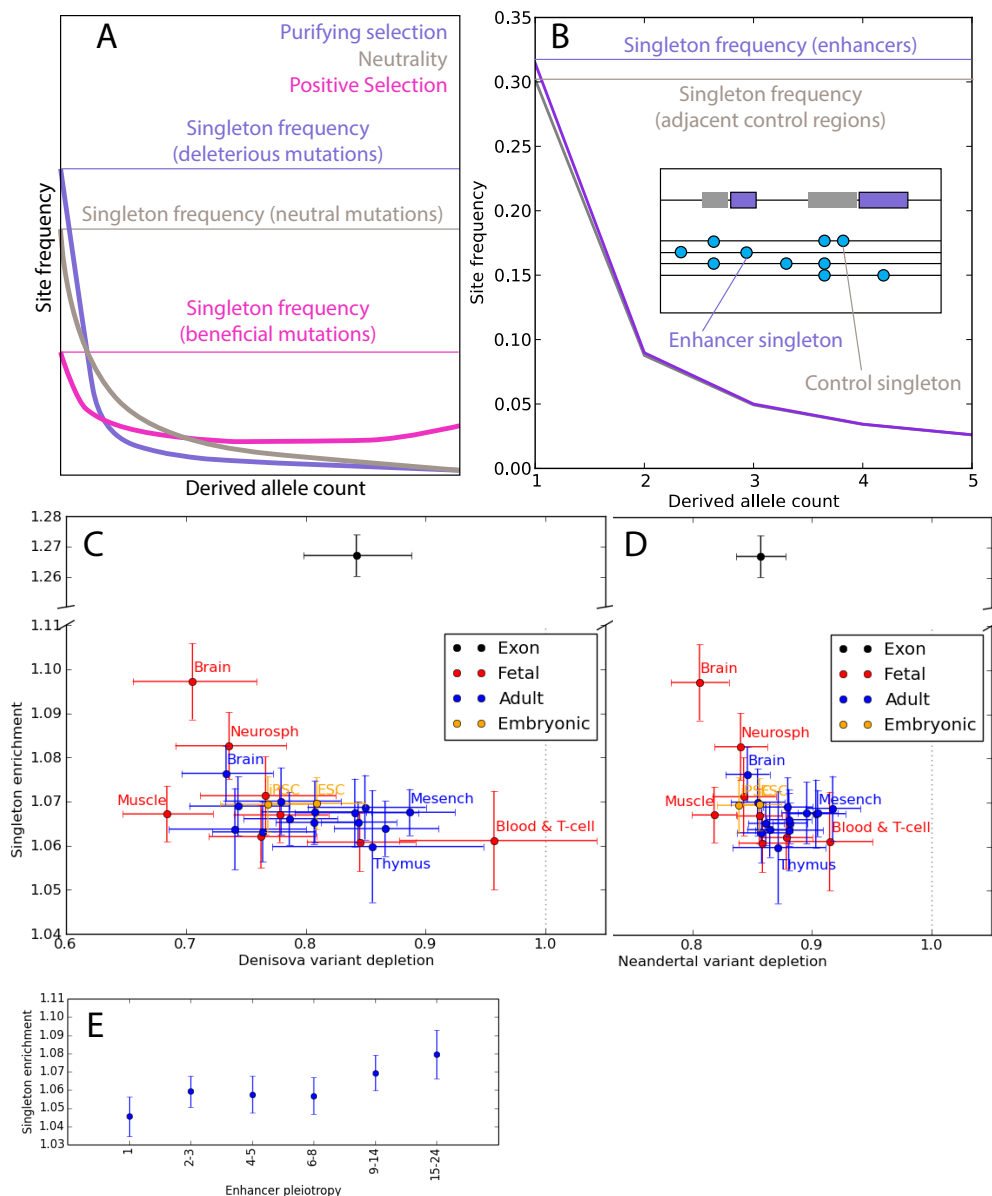


Figure 5: A. Theory predicts that the site frequency spectrum (SFS) becomes skewed toward rare variants by the action of purifying selection. B. In African data from the 1000 Genomes project, the enhancer SFS has a higher proportion of singletons compared to control regions adjacent to enhancers. C. Every tissue type's enhancer complement is enriched for singletons compared to adjacent control regions. This comparison of singleton enrichment odds ratios to Denisovan depletion odds ratios shows that fetal brain, neurosphere cells, and adult brain are outliers under stronger constraint. The y axis has been split to accommodate the magnitude of singleton enrichment in exons. Error bars span 2 binomial test standard errors. D. Comparison of the singleton enrichment landscape to the Neandertal depletion landscape. E. Enhancer pleiotropy is negatively correlated with singleton enrichment, though even enhancers of pleiotropy 1 have a singleton enrichment odds ratio significantly greater than 1. All error bars span 95% binomial confidence intervals.

286 variants from enhancers.

287 Two sources of dysfunction are thought to drive selection against archaic introgression:
288 excess deleterious mutation load in inbred Neandertal and Denisovan populations [43, 44] and
289 accumulation of epistatic incompatibilities due to divergent selective landscapes [5, 7, 45].
290 Both forces have the potential to affect enhancers, and our results confer some ability to
291 distinguish between the two. In particular, the weakness of the correlation between archaic
292 allele depletion and singleton enrichment furnishes useful insights into the fitness effect dif-
293 ferences between *de novo* human mutations and young introgressed archaic alleles. This
294 difference appears starkest when comparing enhancers to exons, which are known to evolve
295 more slowly than enhancers over phylogenetic timescales [46, 47, 48], implying that selection
296 acts more strongly against new coding mutations compared to new regulatory mutations.
297 However, despite their different levels of selective constraint against new mutations, exons
298 and enhancers show evidence for selection against archaic alleles (Figure 5C, D), suggest-
299 ing that regulatory effects may have played a significant role in shaping the landscape of
300 Neandertal and Denisovan introgression.

301 When a set of regulatory elements is more depleted of introgression than expected given
302 their level of selective constraint, this suggests that the Neandertal and Denisovan selective
303 landscape may have diverged from the human one in these regions. Fetal muscle enhancers
304 appear to fit this profile, with unremarkable singleton enrichment and phastCons scores but
305 strong depletion of young archaic variants. Archaeological evidence indicates that Nean-
306 dertals had higher muscle mass, strength, and anatomical robustness compared to humans
307 [49, 50], supporting the idea that the two species had different fetal muscle growth optima.
308 We have no direct knowledge of Denisovan muscle anatomy, but the depletion of Denisovan
309 DNA from muscle enhancers may suggest that they shared Neandertals' robust phenotype,
310 assuming that phenotype is mediated by gene regulation in fetal muscle.

311 In contrast to muscle, mutation load is a more attractive candidate cause for the depletion
312 of archaic alleles from brain enhancers. Our conclusion that brain enhancers experience high
313 deleterious mutation rates is bolstered by prior knowledge of many *de novo* mutations in
314 these regions that cause severe developmental disorders [51, 52, 53].

315 Both genetic load and hybrid incompatibilities might drive the correlation we have found
316 between enhancer pleiotropy and archaic allele depletion. Steinrücken, et al. noted that
317 epistatic incompatibilities are most likely to arise in genes with many interaction partners

318 [54]; when a gene is active in multiple tissues, it must function as part of a different expression
319 network in each tissue, which could create additional constraints on enhancers that must
320 coordinate expression correctly in several different contexts. Our results thus imply that
321 introgression is most depleted from enhancers that must function within a variety of cell-
322 specific regulatory networks. We also know that genes expressed in many tissues evolve more
323 slowly than genes expressed in few tissues because they have greater potential for functional
324 tradeoffs [55, 10], and a mutation that disrupts the balance of a functional tradeoff is likely to
325 have a deleterious effect. This idea is corroborated by our finding that pleiotropic enhancers
326 are more constrained. One caveat is that highly pleiotropy enhancers may be the easiest
327 to experimentally identify. If the RoadMap call sets of tissue-specific enhancers contain a
328 higher proportion of false positives, this might inflate our estimate of the correlation between
329 pleiotropy and selective constraint.

330 Both genetic load and epistatic incompatibilities are expected to “snowball” over time,
331 making young archaic variation more likely to be deleterious in hybrids compared to older,
332 high frequency archaic variation. Part of this effect might be due to positive selection on
333 beneficial introgressed alleles that have risen to high frequency in multiple populations.
334 As more methods for inferring admixture tracts are developed, our results underscore the
335 importance of investigating how they might be biased toward young or old archaic variation
336 and using this information to update our understanding of how selection shapes introgression
337 landscapes. Regulatory mutations appear to have created incompatibilities between many
338 species that are already in the advanced stages of reproductive isolation [56, 57, 58, 59], and
339 our results suggest that they also harmed the fitness of human/Neandertal hybrids during the
340 relatively early stages of speciation between these hominids. As more introgression maps and
341 functional genomic data are generated for hybridizing populations of non-model organisms,
342 it should be possible to measure the prevalence of weak regulatory incompatibility in more
343 systems that exist in the early stages of reproductive isolation and test how many of the
344 patterns observed in this study occur repeatedly outside the hominoid speciation continuum.

345 **Acknowledgements**

346 We are grateful to Jonathan Pritchard, Sriram Sankararaman, Josh Schraiber, and mem-
347 bers of the Harris Lab for helpful discussions, and we thank Rasmus Nielsen for manuscript
348 comments. We also thank three anonymous reviewers whose comments greatly improved

349 the manuscript. We acknowledge financial support from the following grants awarded to
350 K.H: NIH grant 1R35GM133428-01, a Burroughs Wellcome Fund Career Award at the Sci-
351 entific Interface, a Searle Scholarship, a Sloan Research Fellowship, and a Pew Biomedical
352 Scholarship.

353 References

- 354 [1] Green, R. E. *et al.* A draft sequence of the Neandertal genome. *Science* **328**, 710–722
355 (2010).
- 356 [2] Prüfer, K. *et al.* The complete genome sequence of a Neanderthal from the Altai
357 mountains. *Nature* **505**, 43–49 (2014).
- 358 [3] Vernot, B. *et al.* Excavating Neanderthal and Denisovan DNA from the genomes of
359 Melanesian individuals. *Science* 10.1126/science.aad9416 (2016).
- 360 [4] Chen, L., Wolf, A., Fu, W., Li, L. & Akey, J. Identifying and interpreting apparent
361 Neandertal ancestry in African individuals. *Cell* **180**, 677–687 (2020).
- 362 [5] Sankararaman, S. *et al.* The genomic landscape of Neanderthal ancestry in present-day
363 humans. *Nature* **507**, 354–357 (2014).
- 364 [6] Vernot, B. & Akey, J. M. Resurrecting surviving neandertal lineages from modern
365 human genomes. *Science* **343**, 1017–1021 (2014).
- 366 [7] Sankararaman, S., Mallick, S., Patterson, N. & Reich, D. The combined landscape
367 of Denisovan and Neanderthal ancestry in present-day humans. *Current Biology* **26**,
368 1241–1247 (2016).
- 369 [8] King, M. & Wilson, A. Evolution at two levels in humans and chimpanzees. *Science*
370 **188**, 107–116 (1975).
- 371 [9] Enard, W. *et al.* Intra- and interspecific variation in primate gene expression patterns.
372 *Science* **296**, 340–343 (2002).
- 373 [10] Wray, G. The evolutionary significance of *cis*-regulatory mutations. *Nature Reviews*
374 *Genetics* **8**, 206–216 (2007).

- 375 [11] Dannemann, M., Prüfer, K. & Kelso, J. Functional implications of Neanderthal intro-
376 gression in modern humans. *Genome Biology* **18**, 61 (2017).
- 377 [12] McCoy, R., Wakefield, J. & Akey, J. Impacts of Neanderthal-introgressed sequences on
378 the landscape of human gene expression. *Cell* **168**, 916–927 (2017).
- 379 [13] Castellano, S. *et al.* Patterns of coding variation in the complete exons of three Nean-
380 derthals. *Proc Natl Acad Sci USA* **111**, 6666–6671 (2014).
- 381 [14] Hahn, M. Detecting natural selection on *cis*-regulatory dna. *Genetica* **129**, 7–18 (2007).
- 382 [15] Long, H., Prescott, S. & Wysocka, J. Ever-changing landscapes: transcriptional en-
383 hancers in development and evolution. *Cell* **167**, 1170–1187 (2016).
- 384 [16] Wong, W. & Nielsen, R. Detecting selection in noncoding regions of nucleotide se-
385 quences. *Genetics* **167**, 949–958 (2004).
- 386 [17] Torgerson, D. *et al.* Evolutionary processes acting on candidate *cis*-regulatory regions
387 in humans inferred from patterns of polymorphism and divergence. *PLoS Genetics* **5**,
388 e1000592 (2009).
- 389 [18] Ward, L. & Kellis, M. Evidence of abundant purifying selection in humans for recently
390 acquired regulatory functions. *Science* **337**, 1675–1678 (2012).
- 391 [19] Smith, J., McManus, K. & Fraser, H. A novel test for selection on *cis*-regulatory
392 elements reveals positive and negative selection acting on mammalian transcriptional
393 enhancers. *Molecular Biology and Evolution* **30** (2013).
- 394 [20] Arbiza, L. *et al.* Genome-wide inference of natural selection on human transcription
395 factor binding sites. *Nature Genetics* **45**, 723–729 (2013).
- 396 [21] Huerta-Sánchez, E. *et al.* Altitude adaptation in Tibetans caused by introgression of
397 Denisovan-like DNA. *Nature* **512**, 194–197 (2014).
- 398 [22] Prabhakar, S. *et al.* Human-specific gain of function in a developmental enhancer.
399 *Science* **321**, 1346–1350 (2008).

- 400 [23] Capra, J., Erwin, G., McKinsey, G., Rubenstein, J. & Pollard, K. Many human ac-
401 celerated regions are developmental enhancers. *Phil Trans R Soc B* **368**, 20130023
402 (2013).
- 403 [24] Rinker, D. *et al.* Neanderthal introgression reintroduced functional alleles lost in the
404 human out of Africa bottleneck. *bioRxiv preprint* doi.org/10.1101/533257 (2019).
- 405 [25] Silvert, M., Quintana-Murci, L. & Rotival, M. Impact and evolutionary determinants of
406 Neanderthal introgression on transcriptional and post-transcriptional regulation. *The*
407 *American Journal of Human Genetics* **104**, 1241–1250 (2019).
- 408 [26] Mallick, S. *et al.* The Simons Genome Diversity Project: 300 genomes from 142 diverse
409 populations. *Nature* **538**, 201–206 (2016).
- 410 [27] McVicker, G., Gordon, D., Davis, C. & Green, P. Widespread genomic signatures of
411 natural selection in hominid evolution. *PLoS Genetics* **5**, e1000471 (2009).
- 412 [28] Enard, D. & Petrov, D. Evidence that RNA viruses drove adaptive introgression between
413 Neanderthals and modern humans. *Cell* **175**, 360–371 (2018).
- 414 [29] Roadmap Epigenomics Consortium. Integrative analysis of 111 reference human
415 epigenomes. *Nature* **518**, 317–330 (2015).
- 416 [30] Sabarinathan, R., Mularoni, L., Deu-Pons, J., Gonzalez-Perez, A. & Lopez-Bigas, N.
417 Nucleotide excision repair is impaired by binding of transcription factors to DNA. *Nature*
418 **532**, 264–267 (2016).
- 419 [31] Kaiser, V., Taylor, M. & Semple, C. Mutational biases drive elevated rates of substitu-
420 tion at regulatory sites across cancer types. *PLoS Genetics* **12**, e1006207 (2016).
- 421 [32] Quach, H. *et al.* Genetic adaptation and Neandertal admixture shaped the immune
422 system of human populations. *Cell* **167**, 643–656 (2016).
- 423 [33] Nédélec, Y. *et al.* Genetic ancestry and natural selection drive population differences
424 in immune responses to pathogens. *Cell* **167**, 657–669 (2016).
- 425 [34] Dannemann, M., Andrés, A. & Kelso, J. Introgression of Neanderthal- and Denisovan-
426 like haplotypes contributes to adaptive variation in human toll-like receptors. *American*
427 *Journal of Human Genetics* **98**, 22–33 (2016).

- 428 [35] Browning, S., Browning, B., Zhou, Y., Tucci, S. & Akey, J. Analysis of human sequence
429 data reveals two pulses of archaic Denisovan admixture. *Cell* **173**, 53–61 (2018).
- 430 [36] Reich, D. *et al.* Genetic history of an archaic hominin group from Denisova Cave in
431 Siberia. *Nature* **468**, 1053–1060 (2010).
- 432 [37] Slon, V. *et al.* The genome of the offspring of a Neanderthal mother and a Denisovan
433 father. *Nature* **561**, 113–116 (2018).
- 434 [38] Sawyer, S. & Hartl, D. Population genetics of polymorphism and divergence. *Genetics*
435 **132**, 1161–1176 (1992).
- 436 [39] Boyko, A. *et al.* Assessing the evolutionary impact of amino acid mutations in the
437 human genome. *PLoS Genetics* **4**, e1000083 (2008).
- 438 [40] Griffiths, R. The frequency spectrum of a mutation, and its age, in a general diffusion
439 model. *Theor Pop Biol* **64**, 241–251 (2003).
- 440 [41] Meunier, J. & Duret, L. Recombination drives the evolution of GC-content in the human
441 genome. *Mol Biol Evol* **21**, 984–990 (2004).
- 442 [42] Fish, A., Chen, L. & Capra, J. Gene regulatory enhancers with evolutionarily conserved
443 activity are more pleiotropic than those with species-specific activity. *Genome Biology*
444 *and Evolution* **9**, 2615–2625 (2017).
- 445 [43] Harris, K. & Nielsen, R. The genetic cost of Neanderthal introgression. *Genetics* **203**,
446 881–891 (2016).
- 447 [44] Juric, I., Aeschbacher, S. & Coop, G. The strength of selection against Neanderthal
448 introgression. *PLoS Genetics* **12**, e1006340 (2016).
- 449 [45] Schumer, M. *et al.* Natural selection interacts with recombination to shape the evolution
450 of hybrid genomes. *Science* **360** (2018).
- 451 [46] Stone, J. & Wray, G. Rapid evolution of *cis*-regulatory sequences via local point muta-
452 tions. *Molecular Biology and Evolution* **18**, 1764–1770 (2001).
- 453 [47] MacArthur, S. & Brookfield, J. Expected rates and modes of evolution of enhancer
454 sequences. *Molecular Biology and Evolution* **21**, 1064–1073 (2004).

- 455 [48] Nord, A. *et al.* Rapid and pervasive changes in genome-wide enhancer usage during
456 mammalian development. *Cell* **155**, 1521–1531 (2013).
- 457 [49] Ruff, C., Trinkaus, E. & Holliday, T. Body mass and encephalization in Pleistocene
458 *Homo*. *Nature* **387**, 173–176 (1997).
- 459 [50] Churchill, S. Bioenergetic perspectives on Neanderthal thermoregulatory and activity
460 budgets. In Hublin, J., Harvati, K. & Harrison, T. (eds.) *Neanderthals Revisited: New*
461 *Approaches and Perspectives*, 113–133 (Springer, Dordrecht, 2006).
- 462 [51] Gulsuner, S. *et al.* Spatial and temporal mapping of *de novo* mutations in schizophrenia
463 to a fetal prefrontal cortical network. *Cell* **154**, 518–529 (2013).
- 464 [52] Turner, T. *et al.* Genomic patterns of de novo mutation in simplex autism. *Cell* **171**,
465 710–722 (2017).
- 466 [53] Short, P. *et al.* *De novo* mutations in regulatory elements in neurodevelopment disorders.
467 *Nature* **555**, 611–616 (2018).
- 468 [54] Steinrücken, M., Spence, J., Kamm, J., Wiczorek, E. & Song, Y. Model-based detection
469 and analysis of introgressed Neanderthal ancestry in modern humans. *Molecular Ecology*
470 **27**, 3873–3888 (2018).
- 471 [55] Khaitovich, P. *et al.* Parallel patterns of evolution in the genomes and transcriptomes
472 of humans and chimpanzees. *Science* **309**, 1850–1854 (2005).
- 473 [56] Coolon, J., McManus, C., Stevenson, K., Graveley, B. & Wittkopp, P. Tempo and
474 model of regulatory evolution in *Drosophila*. *Genome Research* **24**, 797–808 (2014).
- 475 [57] Turner, L., White, M., Tautz, D. & Payseur, B. Genomic networks of hybrid sterility.
476 *PLoS Genetics* **10**, e1004162 (2014).
- 477 [58] Mack, K., Campbell, P. & Nachman, M. Gene regulation and speciation in house mice.
478 *Genome Research* **26**, 451–461 (2016).
- 479 [59] Lewis, J., van der Burg, K., Mazo-Vargas, A. & Reed, R. ChIP-Seq-Annotated *Helico-*
480 *nius erato* genome highlights patterns of *cis*-regulatory evolution in lepidoptera. *Cell*
481 *reports* **16**, 2855–2863 (2016).

482 **Data Availability Statement**

483 All datasets analyzed here are publicly available at the following websites:

484

CRF Introgression Calls	https://sriramlab.cass.idre.ucla.edu/ public/sankararaman.curbio.2016/summaries.tgz
SGDP	https://www.simonsfoundation.org/ simons-genome-diversity-project/
RoadMap	https://personal.broadinstitute.org/meuleman/reg2map/ HoneyBadger2_release/
1000 Genomes Phase 3	http://www.1000genomes.org/category/phase-3/

485

486 **Code availability statement**

487 Summary data files and custom python scripts for reproducing the paper's main figures are
488 available at <https://github.com/kelleyharris/hominin-enhancers/>.

489 **Author contribution statement**

490 N.T. and K.H. conceived and designed the project. N.T., R.A., and K.H. performed the
491 analyses. K.H. wrote the paper.

492 **Methods**

493 **Extraction of Neandertal and Denisovan variant sets**

494 Neandertal and Denisovan variant call sets were downloaded from <https://sriramlab.cass.idre.ucla.edu/public/sankararaman.curbio.2016/summaries.tgz>. These files classify a haplotype
495 as archaic if it is classified as archaic with $\geq 50\%$ probability by the conditional random
496 field analyses reported in [7]. Using these summaries, we classify a variant as archaic if 100%
497 of the haplotypes on which it appears are classified as such. Unless otherwise stated, all
498 Neandertal and Denisovan variants are obtained from the respective summary call set “2,”
499 which we refer to in the text as the proximal call sets. To construct the distal Neandertal call
500 set analyzed in Figure 4, we included all variants from Neandertal Set 1 except any variants
501 that also appeared in Neandertal Set 1 or Denisovan Set 1. Similarly, the distal Denisovan
502 call set included all variants present in Denisovan Set 1 except those variants also present in
503 Neandertal Set 2 or Denisovan Set 2. Chromosome X was excluded given its unique system-
504 atic depletion of Neandertal and Denisovan variants. Across SGDP populations, the number
505 of SNPs identified as Neandertal in origin ranges from 109,253 (in West Eurasia) to 233,013
506 (in South Asia). The number of introgressed Denisova SNPs ranges from 6,437 (in West
507 Eurasia) to 68,061 (in Oceania).
508

509 **Classifying enhancers by tissue type and pleiotropy number**

510 Cell lines were classified into tissue types using the tissue assignment labels from the July
511 2013 RoadMap data compendium, available at https://personal.broadinstitute.org/meuleman/reg2map/HoneyBadger2_release/DNase/p10/enh/state_calls.RData. When-
512 ever a tissue type contained both fetal and adult cell lines, we further subdivided that tissue
513 type into “Adult” and “Fetal.” We then computed a pleiotropy number for each enhancer
514 by counting the number of distinct tissue type labels in the cell lines where that enhancer
515 is annotated as active. Three separate states are used to denote enhancer activity in the
516 honey badger model: states 6, 7, and 12 denote genic enhancers, enhancers, and bivalent
517 enhancers, respectively, and we could each of these states as equivalent evidence of enhancer
518 activity. Fetal and adult tissue types are counted as distinct tissues for the purpose of this
519 computation.
520

521 **Testing for depletion of archaic variation relative to matched con-** 522 **trol variation**

523 To estimate the strength of background selection experienced by human genomic loci, B-
524 statistic values ranging on a scale from 1 to 1000 were downloaded at [http://www.phrap.org/](http://www.phrap.org/software_dir/mcvicker_dir/bkgd.tar.gz)
525 `software_dir/mcvicker_dir/bkgd.tar.gz`. We quantized these values by rounding them
526 down to the nearest multiple of 50 B-statistic units, then lifted them over from hg18 coordi-
527 nates to hg19 coordinates. Each SNP in the SGDP data was assigned the B statistic value
528 of the closest site annotated by McVicker, et al.

529 Our tests for depletion of archaic variation are computed relative to non-archaic control
530 SNPs that have the same joint distribution of allele frequency and B statistic as the SNPs an-
531 notated as archaic in origin. See the next section, “Detailed sampling procedure for matched
532 control SNPs”, for more information on how these matched control sets are obtained.

533 Assume that \mathcal{A} is a set of A archaic SNPs and \mathcal{C} is a set of $2 \times A$ matched controls. (We
534 chose to sample $2A$ controls rather than A controls to reduce the stochasticity of the control
535 set and decrease the size of the confidence intervals on all computed odds ratios). To test
536 whether archaic variation of this type is enriched or depleted in a set \mathcal{G} of genomic regions,
537 we start by counting the number A_G of archaic SNPs contained in \mathcal{G} and the number C_G of
538 control SNPs contained in \mathcal{G} . We say that this type of archaic variation is depleted from \mathcal{G}
539 if the odds ratio $(A_G/(A - A_G))/(C_G/(2A - C_G))$ is less than 1.

540 To assess the significance of any enrichment or depletion we measure, we ask whether
541 the corresponding log odds ratio $\log(A_G) + \log(2A - C_G) - \log(A - A_G) - \log(C_G)$ is
542 more than two standard errors away from zero. The standard error of this log odds ra-
543 tio is $\sqrt{1/A_G + 1/(2A - C_G) + 1/C_G + 1/(A - A_G)}$. In each forest plot presented in the
544 manuscript, this formula was used to draw error bars that span two standard errors in each
545 direction.

546 **Detailed sampling procedure for matched control SNPs**

547 For each archaic SNP set (Neandertal 1, Neandertal 2, Denisovan 1, and Denisovan 2) and
548 each population p , we counted the number $A_p(b, c)$ of alleles with B-statistic value b and
549 derived allele count c in population p , counting the allele as archaic if all derived alleles
550 were annotated as present on archaic haplotypes in the relevant call set of population p .
551 We then counted the number $N_p(b, c)$ of non-archaic alleles with B-statistic b and derived

552 allele count c . In order for a SNP to count as non-archaic, none of its derived alleles could
553 be present on a haplotype from population p that was called as archaic in either call set
554 1 or call set 2. A set $\mathcal{C}_p(b, c)$ of $2 \times A_p(b, c)$ control SNPs was then sampled uniformly at
555 random without replacement from the $N_p(b, c)$ control candidate SNPs. In the rare event
556 that $N_p(b, c) < 2 \times A_p(b, c)$, the control set was defined to be the entire set $N_p(b, c)$ and an
557 extra $2 \times A_p(b, c) - N_p(b, c)$ SNPs from the control set were chosen uniformly at random to
558 be counted twice in all analyses.

559 Several analyses in the paper are performed on a merged set of archaic variation compiled
560 across populations. To form the archaic SNP set $\mathcal{A}(b, c)$, we merged together the archaic SNP
561 sets $\mathcal{A}_p(b, c)$ across all populations p . For each site where the derived allele was present in two
562 or more populations, it was randomly assigned one population of origin. This population
563 assignment process yielded new archaic allele counts $A'_p(b, c)$ that might be less than the
564 counts $A_p(b, c)$ due to the deletion of duplicate SNPs. For each population p , we sampled
565 $2 \times A'_p(b, c)$ control SNPs from population p as before and merged all of these control sets
566 together to obtain a merged control set $\mathcal{C}(b, c)$. In the unlikely event that a single control
567 allele is sampled in two or more populations, this control SNP will simply be counted two
568 or more times during downstream analyses.

569 To obtain sets of distal archaic SNPs and controls, we must be careful about how we
570 subtract call set 2 from call set 1. We want to sample control SNPs such that no control
571 SNP is part of call set 2 for any archaic species in any population. To achieve this, the set
572 of distal Denisovan SNPs $\mathcal{A}^{(D1-2)}(b, c)$ is defined as the set of all SNPs that are present in
573 Denisovan call set 1 $\mathcal{A}^{(D1)}(b, c)$ but absent from both the Denisovan call set 2 $\mathcal{A}^{(D2)}(b, c)$ and
574 the Neandertal call set 2 $\mathcal{A}^{(N2)}(b, c)$. To generate the corresponding control set $\mathcal{C}^{(D1-2)}(b, c)$,
575 we first look within each population to generate the superset of matched control SNPs
576 $\mathcal{N}_p^{(D1-2)}(b, c)$. $\mathcal{N}_p^{(D1-2)}(b, c)$ is defined as the set of all SNPs present in population p in
577 Denisovan call set 1 ($\mathcal{N}_p^{(D1)}(b, c)$) but absent from the population-merged sets of nonarchaic
578 variants from Neandertal Set 2 ($\mathcal{N}^{(N2)}(b, c)$) plus Denisovan Set 2 ($\mathcal{N}^{(D2)}(b, c)$). Once we
579 have the population-specific candidate control sets $\mathcal{N}_p^{(D1-2)}(b, c)$, we randomly assign each
580 archaic SNP from $\mathcal{A}^{(D1-2)}(b, c)$ to one of the populations where the derived allele is called as
581 archaic, obtaining population-specific call sets $\mathcal{A}'_p^{(D1-2)}(b, c)$ that each contain $A'_p^{(D1-2)}(b, c)$
582 SNPs. As described earlier, we sample $2 \times A'_p^{(D1-2)}(b, c)$ control SNPs uniformly at random
583 from each set $\mathcal{N}_p^{(D1-2)}(b, c)$ and merge these control sets together to obtain a merged set of

584 distal controls C_p^{D1-2} .

585 **Sampling an alternate set of controls to approximate the clustering** 586 **and LD structure of introgressed variation**

587 The archaic variants present in the human population do not have independent demographic
588 and selective histories, but are in many cases organized into linked archaic haplotypes. To
589 measure whether this LD structure might affect the apparent depletion of archaic alleles from
590 enhancers, we sampled an alternate set of control SNPs whose LD structure is more similar
591 to the LD structure of the introgressed SNPs. LD has the effect of organizing introgressed
592 SNPs into clusters of close-together variants that have similar allele frequencies, and such
593 clustering could increase the probability that a short enhancer sequence might fall into a gap
594 between introgressed SNPs.

595 To enable sampling of control SNPs in a way that matches the clustering of archaic SNPs,
596 we first organized the introgressed SNPs into blocks, considering two SNPs to be part of the
597 same block if they are less than 20 kb apart and have minor allele counts that differ by at
598 most 1. After organizing the archaic SNPs into these blocks, we counted blocks of control
599 SNPs from the same population VCF that had approximately the same allele frequency and
600 B statistic value. In order to find enough matched control blocks, we relaxed the assumption
601 that archaic and control SNPs should have exactly the same allele frequency and B statistic.
602 Instead, we binned minor allele count into log-2 spaced bins (minor allele count 1, 2, 3-4,
603 5-8, 9-16, 17+) and required each control SNPs cluster to match the minor allele count bins
604 of the matched archaic cluster. Specifically, given a block of k archaic SNPs that we infer
605 to be a haplotype block, we assign the minor allele count bin of that block to be the most
606 common bin occupied by the k SNPs. We assigned the B statistic of the block to be the
607 median B statistic of the k SNPs. We then counted the number of blocks of k consecutive
608 non-introgressed SNPs that had the same minor allele count (plus or minus 1), the same
609 median B statistic, and whose genomic span in base pairs was within a factor of 2 of the
610 span in base pairs of the archaic SNP set. We selected one of these blocks uniformly at
611 random to be the control SNP block matched to the archaic SNP block.

612 **Quantifying singleton enrichment in the 1000 Genomes site fre-** 613 **quency spectrum**

614 Let \mathcal{G} be a set of enhancers or other genomic regions. To test whether \mathcal{G} is under stronger
615 purifying selection than its immediate genomic neighborhood, we compared its site frequency
616 spectrum (SFS) to the SFS of a region set \mathcal{G}' defined as follows: \mathcal{G} can always be defined
617 as a collection of genomic intervals $\{(g_1^{(1)}, g_1^{(2)}), \dots, (g_n^{(1)}, g_n^{(2)})\}$, where each $(g_k^{(1)}, g_k^{(2)})$ is a
618 pair of genomic coordinates delineating a piece of DNA contained entirely within the set \mathcal{G} .
619 We define \mathcal{G}' to be the collection of genomic intervals $\{(2 \times g_k^{(1)} - g_k^{(2)}, g_k^{(k)})\}$, i.e. the set of
620 intervals immediately adjacent on the left to the intervals that make up \mathcal{G} . (We are slightly
621 abusing notation here by failing to note that different chromosomes have different coordinate
622 systems).

623 We computed folded site frequency spectra for \mathcal{G} and \mathcal{G}' using the African individuals
624 in the 1000 Genomes Phase 3 VCF, excluding SNPs that do not pass the VCF's default
625 quality filter. Let S_G and $S_{G'}$ be the numbers of singletons that fall in into the regions \mathcal{G} and
626 \mathcal{G}' , respectively, and let N_G and $N_{G'}$ be the numbers of non-singleton variants that fall into
627 these regions. We say that \mathcal{G} is enriched for singletons if the odds ratio $(S_G/N_G)/(S_{G'}/N_{G'})$
628 is greater than 1. To assess the significance of any enrichment or depletion, we use the
629 fact that the standard error of this binomial test is $\sqrt{1/S_G + 1/N_G + 1/S_{G'} + 1/N_{G'}}$. All
630 singleton enrichment plots in this manuscript contain error bars that span 2 standard errors
631 above and below the estimated odds ratio.

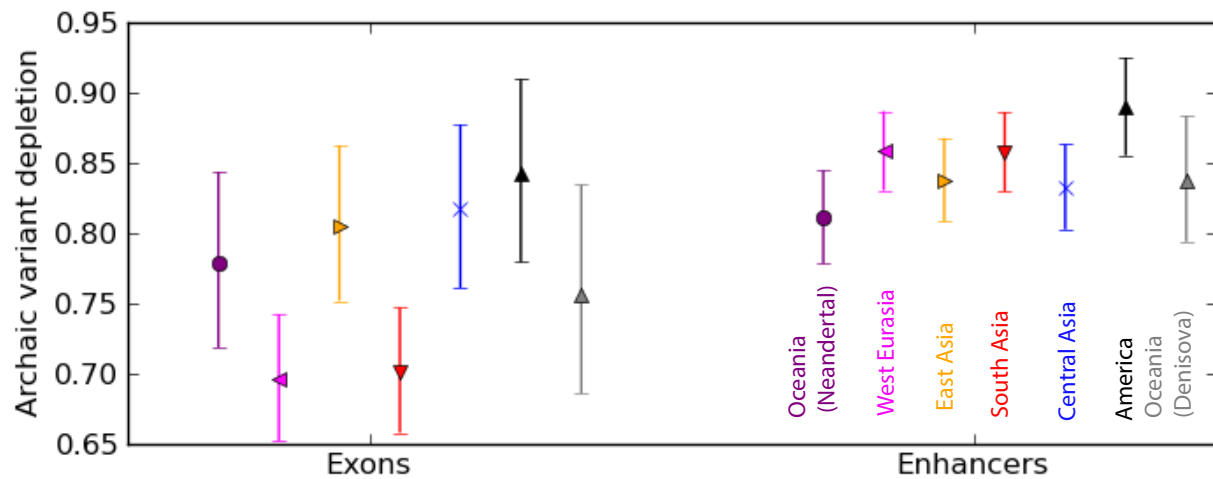


Figure S1.1 We replicated the analysis from Figure 1B using archaic SNPs and controls sampled to match the clustering induced by LD structure. The depletion of archaic SNPs from exon and enhancers is nearly identical to the depletion measured using controls not sampled to match the spatial clustering of introgressed SNPs.

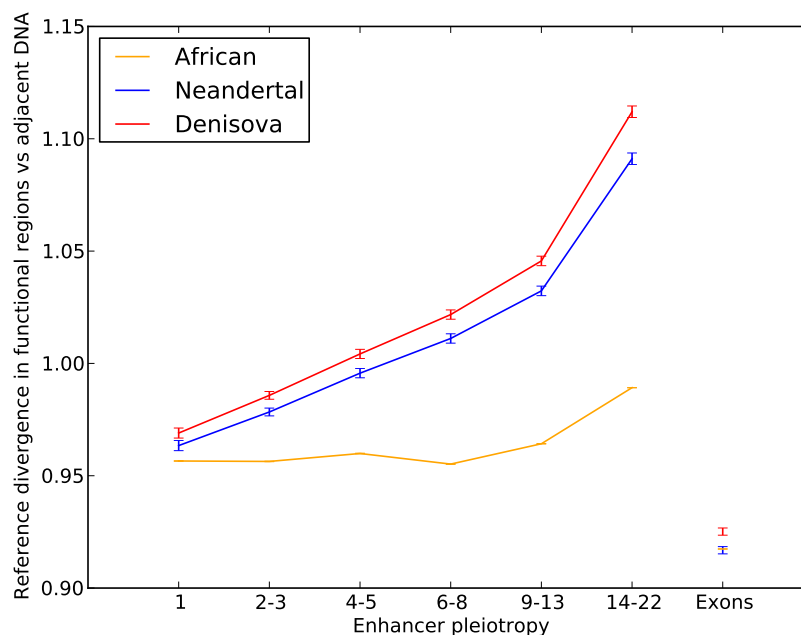


Figure S2.1 If human and archaic genomes were less diverged from each other in high-pleiotropy enhancers than within other regions of the genome, this could in theory explain why introgressed archaic SNPs are depleted from high pleiotropy enhancers. However this plot shows that the opposite pattern is true: human divergence from reference archaic genomes is higher within high-pleiotropy enhancers than within matched sets of enhancer-sized control regions located 3'-adjacent to enhancers in the genome. To see this, we let $\pi_{\text{Nean}}(p)$ be the pairwise divergence between a Neandertal haplotype (averaged between the two haplotypes of the Altai Neandertal reference) and the human reference genome measured across the set of enhancers of pleiotropy p , and let $\pi'_{\text{Nean}}(p)$ be the pairwise divergence between Neandertal and human within the adjacent matched control regions. The line labeled “Neandertal” in the above plot shows $\pi_{\text{Nean}}(p)/\pi'_{\text{Nean}}(p)$ as a function of pleiotropy number p . We also measured the average divergence of the human reference genome from an Altai Denisovan reference haplotype and from the set of African genomes sequenced as part of the 1000 Genomes project. The results, $\pi_{\text{Nean}}(p)/\pi'_{\text{Nean}}(p)$, $\pi_{\text{Deni}}(p)/\pi'_{\text{Deni}}(p)$, and $\pi_{\text{AFR}}(p)/\pi'_{\text{AFR}}(p)$, are plotted together with error bars derived from the binomial approximation to the Bernoulli distribution. Divergence between each pair of genomes is consistently lower in exons compared to adjacent control regions, an observation that is consistent with the conserved nature of exonic sequence. In contrast, enhancers are overall more diverged between populations and species than control regions are, and this acceleration of divergence is positively correlated with enhancer pleiotropy. This correlation is stronger for archaic vs human comparisons than for the African vs human reference genome comparison. In the absence of selection against Neandertal DNA in enhancers, this enrichment of divergence should cause a pattern of archaic SNP enrichment within high-pleiotropy enhancers, not the pattern of depletion that we in fact observe.

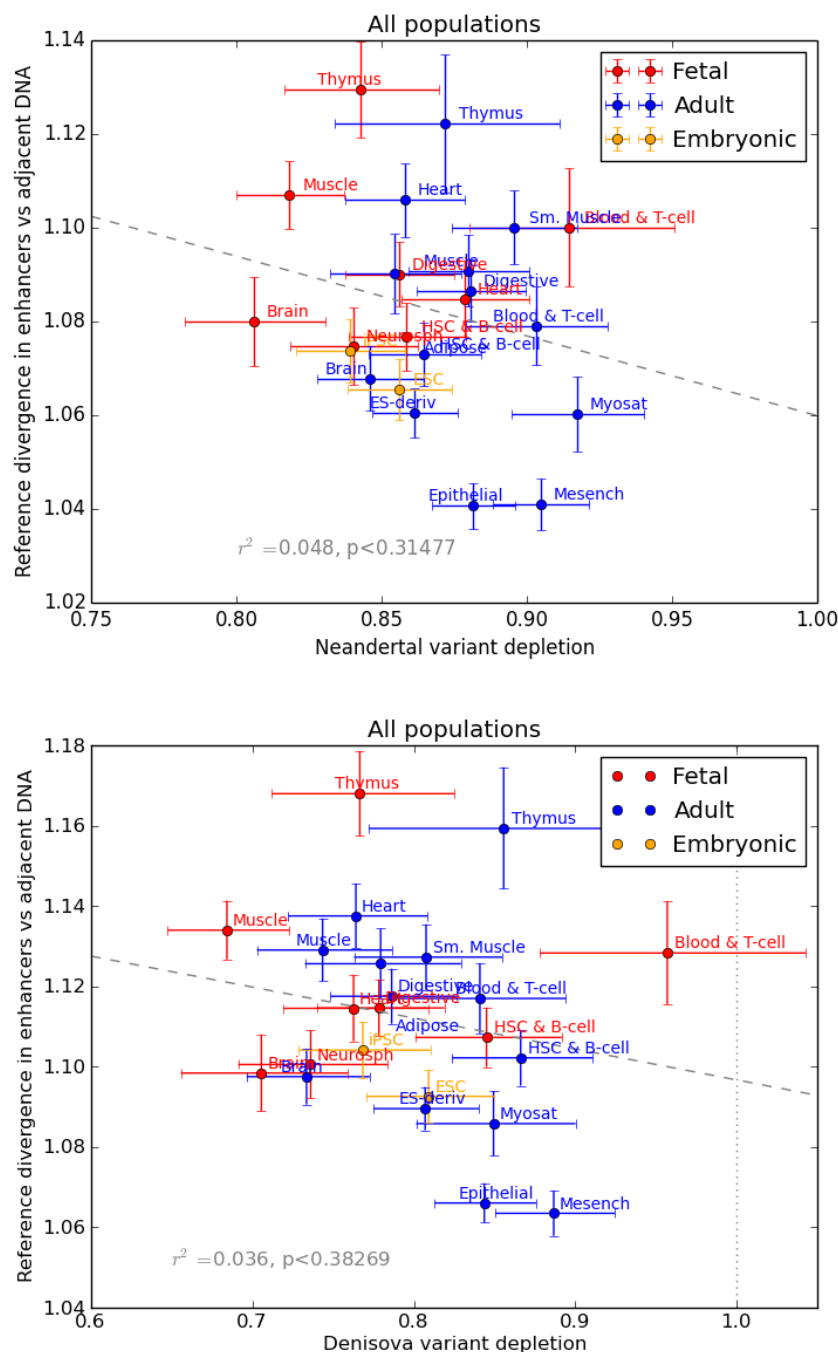


Figure S2.2 Within the set of enhancers active in each cell type, we measured divergence between human and archaic reference genomes and compared it to human/archaic divergence within adjacent matched control regions as described in Figure S2.1. The results are plotted here together with error bars derived from the binomial approximation to the Bernoulli distribution. We see no correlation across tissues between the amount of archaic divergence from the human reference and the degree of archaic allele depletion from enhancers. This absence of correlation suggests that differences between tissues in density of introgressed archaic variants are not driven by regional differences in the degree of divergence between archaic and human genomes.

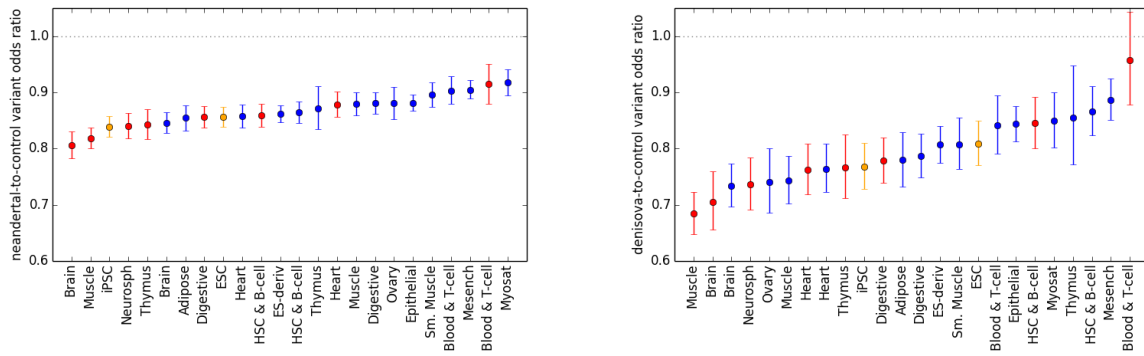


Figure S3.1 These plots show the data from Figure 3 with Neandertal and Denisovan odds ratios on separate plots for clarity.

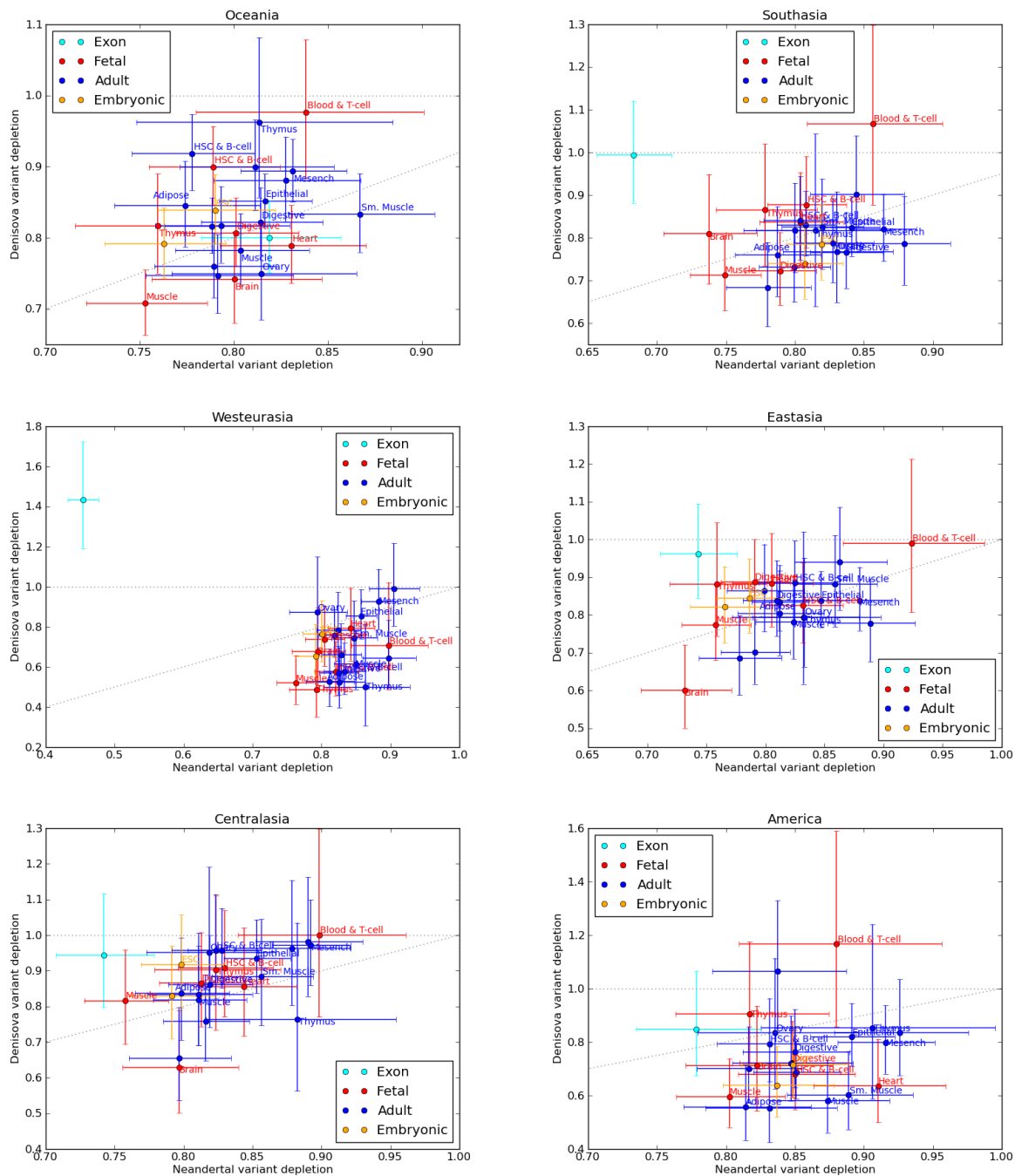


Figure S3.2 These plots show the joint distribution of Neandertal and Denisovan introgression depletion within each SGDP population separately. Although there are differences between populations, particularly since Denisovan introgression is sparse and noisy in general, all show that brain and fetal muscle enhancers are the most depleted of introgression. In most populations the blood & T-cell tissue is least depleted of introgression.

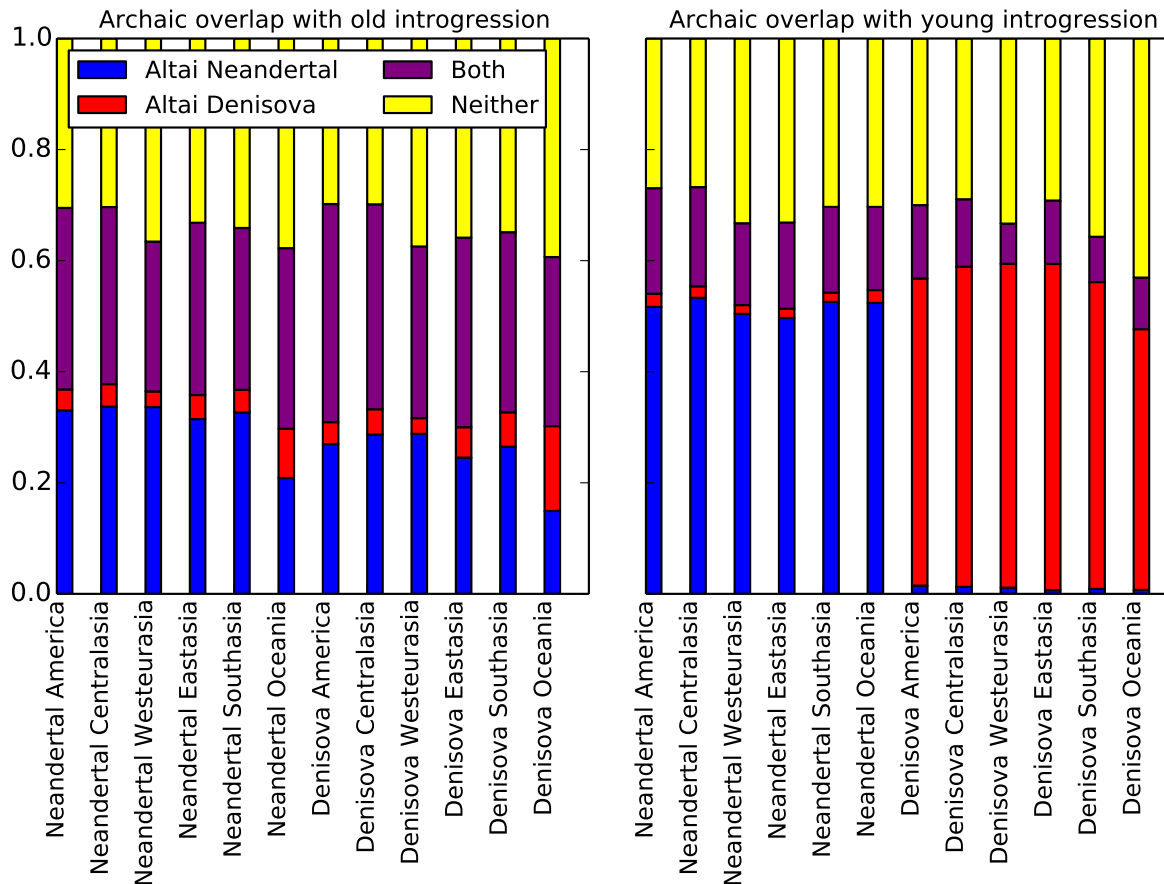


Figure S4.1 For each human SGDP population, this figure shows the fraction of introgressed nonreference alleles that are shared with the Altai Neandertal genome, the Altai Denisova genome, both, or neither. Recall that “young” introgression calls are SNPs that appear in call set 2 generated by Sankararaman, et al. while “old” calls appear in call set 1 for at least one archaic species but not in either set of young calls. In every population, 20% to 30% of old introgressed SNPs are shared with both archaic reference genomes, indicating that these alleles predate the divergence of Neandertals and Denisovans or are at least old enough to have passed between the two species by gene flow. In contrast, only 10% to 20% of young introgressed SNPs are present in both archaic genomes. In each set of young Neandertal introgression calls, over 45% of alleles are shared with the Altai Neandertal but not the Altai Denisovan; conversely, in each set of young Denisovan introgression calls, over 45% of alleles are shared with the Denisovans reference but not the Neandertal reference. Old Neandertal and Denisovan introgression calls look much more similar to each other: each contains 10% to 25% alleles found specifically in the Neandertal reference as well as 2% to 10% alleles found specifically in the Denisovan reference. These patterns of allele sharing support our hypothesis that the old calls are indeed older than the young calls.

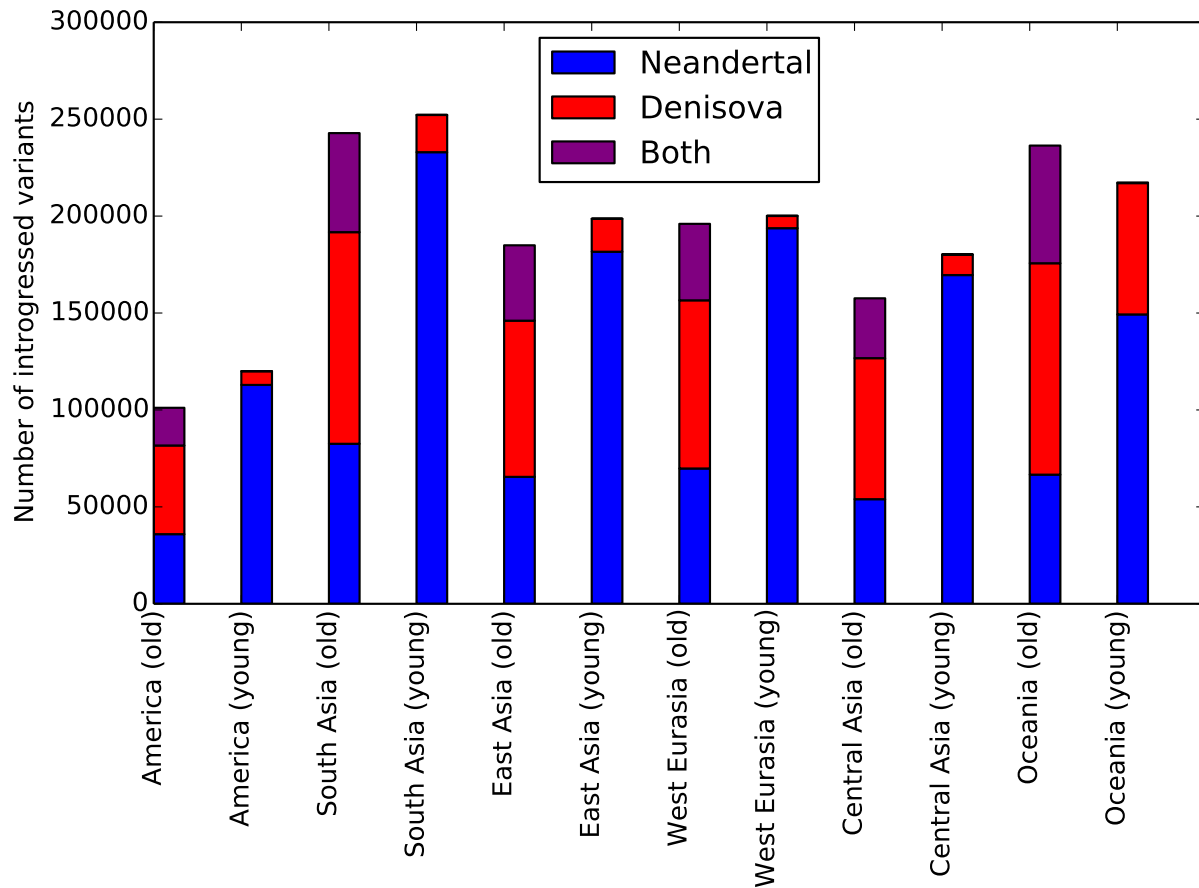


Figure S4.2 This chart shows the number of SNPs in each population that we classify as young versus old, based on their presence in the Sankararaman, et al. call sets 1 versus 2. Each SNP set is further subdivided into SNPs that appear in the Neandertal introgression call set only, the Denisova introgression call set only, or the intersection of both call sets.

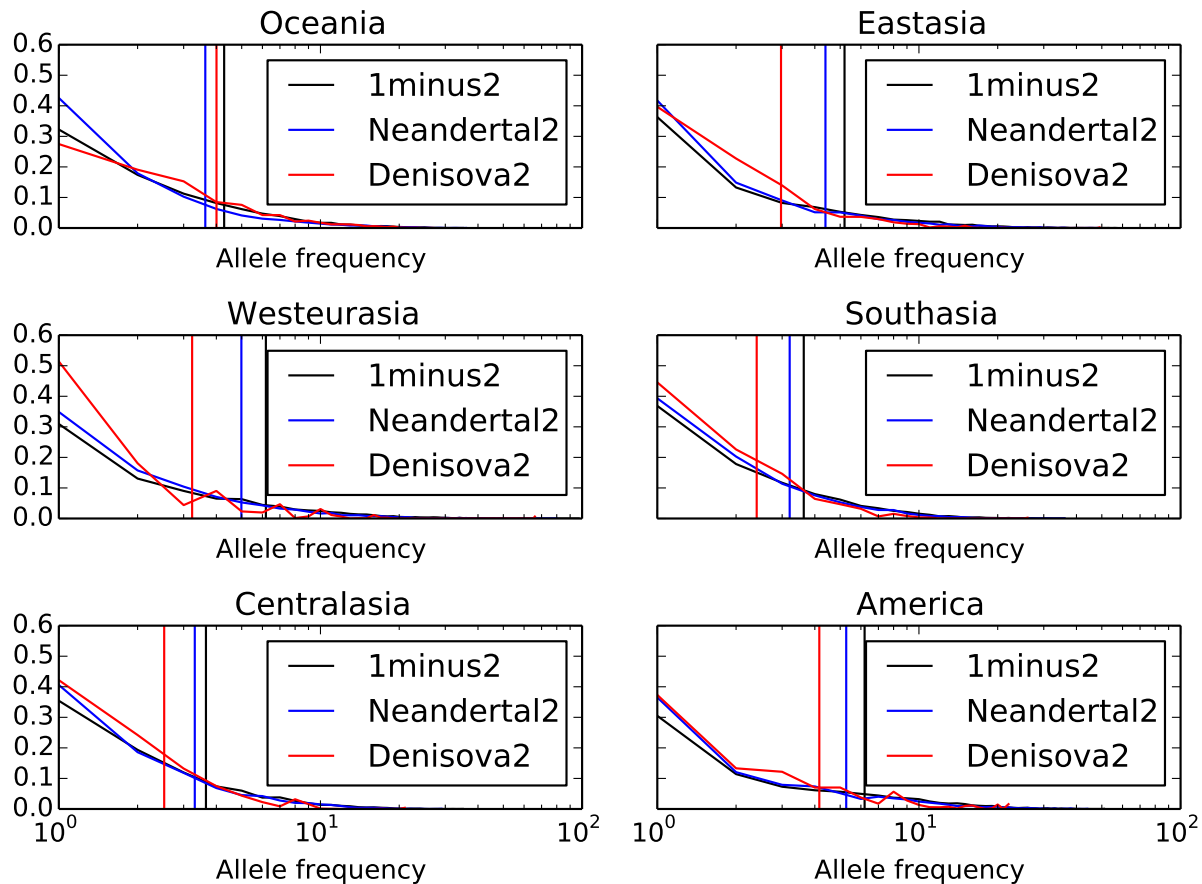


Figure S4.3 For each of the six SGDP populations, this figure shows the site frequency spectra of variants from the conditional random field call sets that we classify as young versus old. For each call set, the corresponding vertical line demarcates the mean allele frequency of that category. In each population, the old “1 minus 2” call set has the highest mean allele frequency, adding support to our hypothesis that these variants are older and/or less deleterious than either population-specific Call Set 2.

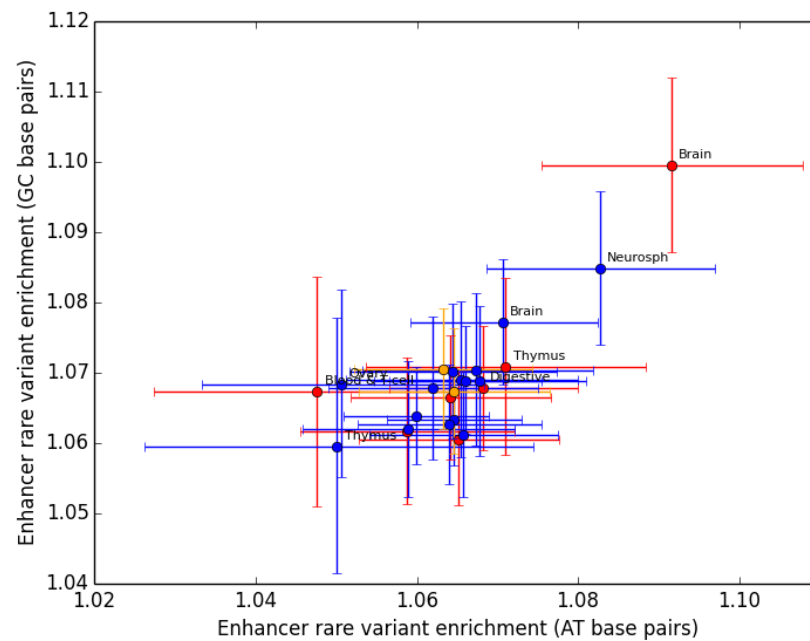


Figure S5.1 This figure was generated by partitioning the site frequency spectrum of each enhancer between SNPs that have GC ancestral alleles and SNPs that have AT ancestral alleles. The site frequency spectra of these two classes of sites are expected to be driven in opposite directions by GC biased gene conversion. However, the finding that brain enhancers are enriched for singletons holds up when we restrict to either GC-ancestral SNPs or AT-ancestral SNPs.

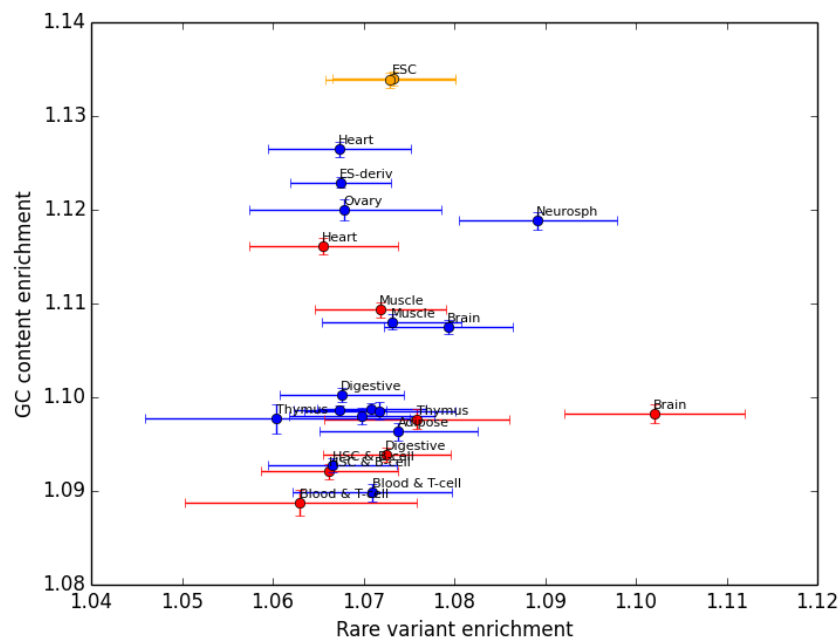


Figure S5.2 Enhancers are enriched for GC base pairs compared to adjacent genomic regions, and the degree of this enrichment varies between tissues. However, there is no correlation across tissues between GC content enrichment and the singleton enrichment that we attribute to purifying selection.

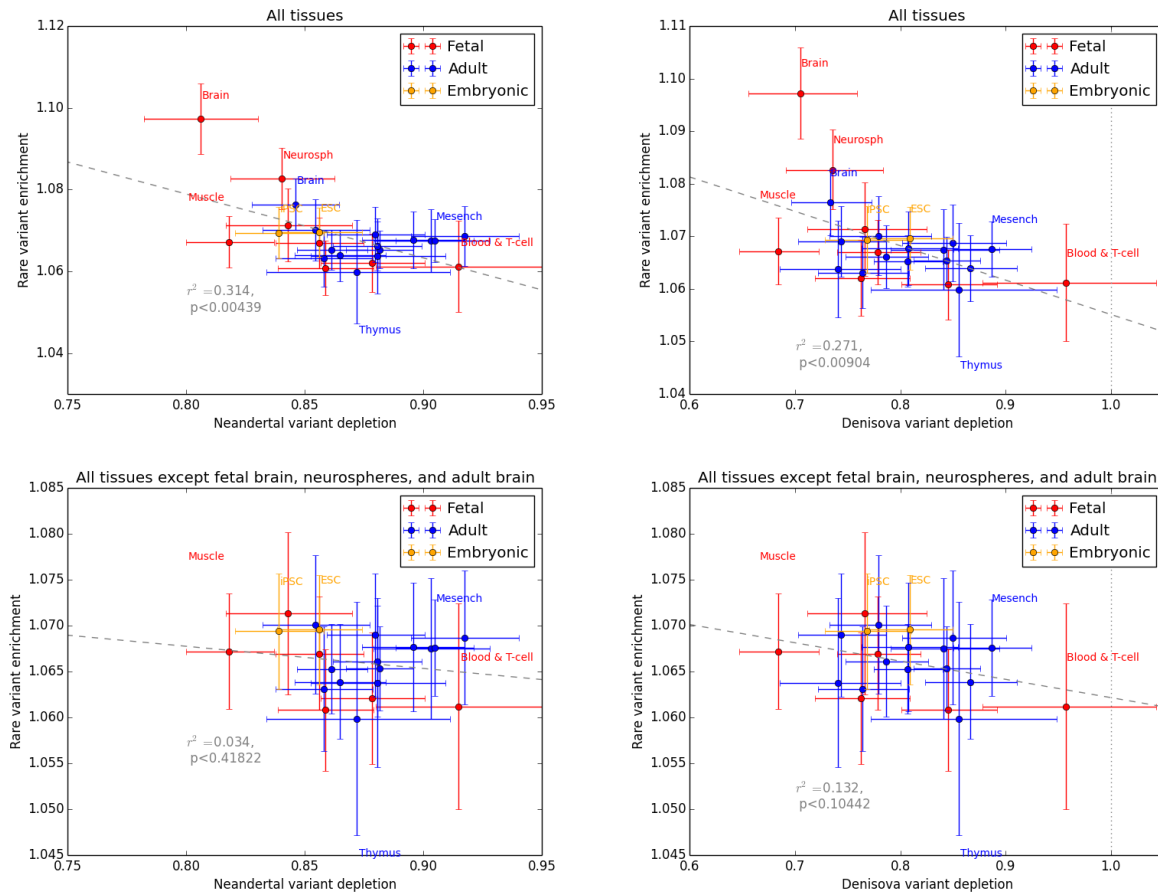


Figure S5.3 Although singleton enrichment is negatively correlated between tissues with both Neandertal and Denisovan variant depletion, the significance of this correlation disappears when all brain related tissues are excluded from the regression.

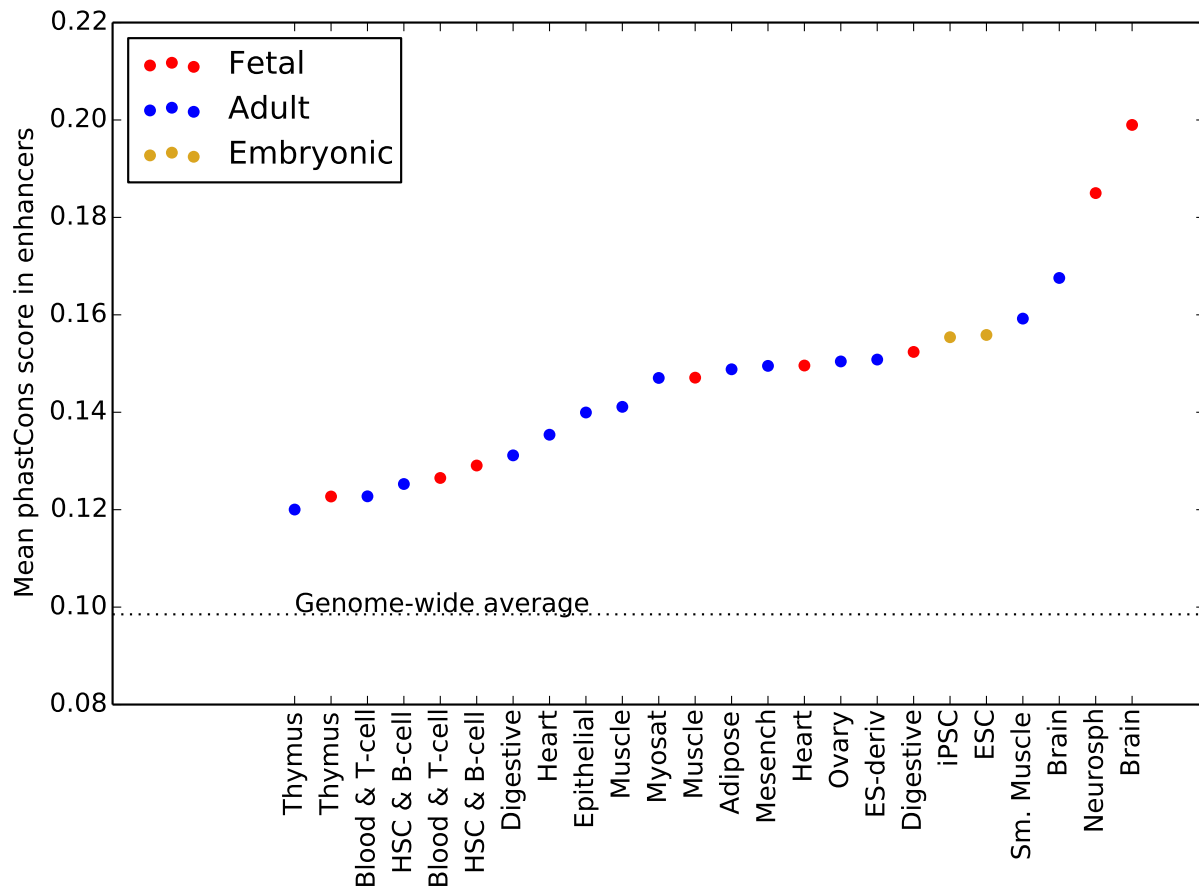


Figure S5.4 Across all tissues, enhancers have a mean phastCons score that is slightly elevated above the genomic mean, indicating that these regions are slightly conserved over phylogenetic timescales. Fetal brain and neurosphere enhancers have a higher mean phastCons score than enhancers active in any other tissues. This result mirrors our findings on the landscape of recent purifying selection as measured by site frequency skew: fetal brain enhancers are more conserved than other regulatory elements, but fetal muscle enhancers are not.